ASME Journal of Electronic Packaging
Online journal at:
https://asmedigitalcollection.asme.org/electronicpackaging

Jonghwan Ha[1]
Mem. ASME
Mechanical Engineering Department,
The State University of New York at Binghamton,
85 Murray Hill Road,
Vestal, NY 13850
e-mail: jha16@binghamton.edu

Yangyang Lai
Mem. ASME
Mechanical Engineering Department,
The State University of New York at Binghamton,
85 Murray Hill Road,
Vestal, NY 13850
e-mail: ylai9@binghamton.edu

Junbo Yang
Mem. ASME
Mechanical Engineering Department,
The State University of New York at Binghamton,
85 Murray Hill Road,
Vestal, NY 13850
e-mail: jyang151@binghamton.edu

Pengcheng Yin
Mem. ASME
Mechanical Engineering Department,
The State University of New York at Binghamton,
85 Murray Hill Road,
Vestal, NY 13850
e-mail: pyin2@binghamton.edu

Seungbae Park
Mem. ASME
Mechanical Engineering Department,
The State University of New York at Binghamton,
85 Murray Hill Road,
Vestal, NY 13850
e-mail: sbpark@binghamton.edu

Effect of Differently Shaped Solder Joints of Chip Resistor on Fatigue Life

As surface mount components shrink in size, smaller apertures on stencils during solder paste printing can lead to uneven solder volume on a single resistor. This can result in the formation of irregular solder shapes, which are often deemed acceptable criterion depending on assembly house. However, such irregularities can potentially introduce variations in the fatigue life of the surface mount component. This study employs experimental and numerical approaches to investigate the reliability of differently shaped SAC305 solder joints on a single chip resistor. Four distinct solder shapes, concave, straight, tiny convex, and convex, are generated using varying volumes of solder paste controlled by uniquely designed apertures on a stencil. Eight pairs of differently shaped solder joints are assembled to hold a chip resistor in place. The test assembly involves R1005 and R0402 soldered with SAC305 and undergoes thermal shock cycling. As a single chip resistor assembly consists of two solder joints connecting termination and pads, the effect of solder volume difference between two solder joints are investigated. The fatigue life corresponds to decrease as the solder volume difference increase as 40%, 80%, and 120%. Conversely, total volume of two solder joints in a single chip resistor increases in scenarios with the same volume difference between two solder joints. Experimental data and finite element analysis lead to a new set of Darveaux's constants specific to this assembly. This study provides guideline to control the solder paste volumes in relation to fatigue life and enables numerical solution using a new Darveaux's constants. [DOI: 10.1115/1.4063058]

1 Introduction

In the recent surface mount technology, small size of chip resistors, such as R1005 and R0402, is not rare and is widely adopted in electronic packages. However, smaller components lead to greater variations of solder volumes on a single component because smaller apertures on a stencil also necessitate. Variations in solder volumes cause inconsistent solder shapes, which disturb the self-alignment characteristics of the surface mount component. This self-alignment failure results in overhung or distorted components since the chip resistor is assembled with two solder joints on a single resistor. Hence, irregularly shaped solder joints can have a significant impact on the reliability of solder joints in terms of thermal and shock domains [1,2].

The formation of solder joints in chip component packages has been widely studied. A simple force model to predict the shape of solder joints has been developed [3]. Additionally, an improved two-dimensional model that accounts for hydrostatic and capillary pressure on the molten solder has been established, using a curved line instead of a straight line for fillet [4]. As the energy in the molten solder, such as surface tension energy, gravitational potential energy, and pressure, reaches an equilibrium state, the molten solder takes on an energy minimized shape. The formation of the solder joint is greatly influenced by solder paste volume and the geometry of the component and pad [5–7].

In previous studies, researchers have investigated the thermal reliability of a solder joint in chip component assemblies subjected

[1]Corresponding author.

Contributed by the Electronic and Photonic Packaging Division of ASME for publication in the Journal of Electronic Packaging. Manuscript received April 1, 2023; final manuscript received July 23, 2023; published online August 17, 2023. Assoc. Editor: Ming-Yi Tsai.

to thermal cycling. Thermal cycling produces stress and strain in the solder joints because of the coefficient of thermal expansion (CTE) mismatch between the solder, component, pad, and printed circuit board (PCB). This leads to the formation of crack that spread through the solder connection. A crack in the solder joint usually starts at the point where the solder meets the pad and propagates throughout the fillet during thermal cycling. Eventually, the crack emerges on the surface of the fillet, and severance in the solder joint is caused completely. Thus, solder joint is not available to play a role in electrical interconnection [8]. Therefore, the distance between the termination of the component and the pad, known as the standoff height, is a critical factor affecting fatigue life. The standoff height can be increased by depositing more solder paste [9,10]. Other investigations concluded that shear stress, which reduces shear strength, is dominated by standoff height and lower standoff height reduces fatigue life [11,12].

Nonetheless, previous studies have limitations due to several simplifications and assumptions made, which may have discrepancies in representing reality. For instance, in surface mount technology, solder paste is applied on the pads through apertures on a stencil, which is properly aligned above the PCB. However, removing the stencil from the PCB during the typical process can result in some solder paste being removed from the pad due to the sidewall in the aperture holding paste [13]. The amount of solder paste, which is not properly transferred, significantly depends on the stencil aperture [14]. This could lead to insufficient solder volumes on pads, particularly in mass production and high-density electronic applications, where various sizes of components share the same stencil for solder paste deposition. Depending on the assembly house and makers, pass/fail criterion of solder paste volume varies with respect to solder joint shape. Generally, $\pm$ 50% volume of solder paste can be determined as pass criterion. However, this discrepancy induces various solder shapes in a single chip resistor, and the reliability of chip resistor assembly failure is highly influenced by the solder joint shape. The question then arises of what happens to thermal reliability in this situation. It is still not yet clearly investigated how they are different in thermal reliability. Hence, it is necessary to consider thermal fatigue life of nonsymmetrical solder joint shapes on a single resistor. By comparing the fatigue life of these assemblies, guidelines for pass/fail criterion of solder paste volume in thermal reliability could be establish and provided to obtain more reliable solder joints.

This study aims thermal reliability of two differently shaped solder joints in a chip resistor under thermal shock cycling. In small chip resistors, it is challenging to predict the solder shape regarding solder volume after the reflow process compared to BGA packages. Therefore, a three-dimensional (3D) model created in Surface Evolver is used to accurately predict the solder joint shape after the reflow process in this study. The study proceeds in two steps. First, four different solder shapes: concave, straight, tiny convex, and convex, are predetermined by inputting various solder paste volumes into a 3D model of Surface Evolver. Second, stencil apertures are designed based on the solder volumes inducing predetermined shapes. Then, two apertures are matched to create eight pairs of differently shaped solder joints on a single resistor. This method enables the successful assembly of a test board with two different shapes holding a single resistor in place. Two types of chip resistors, R1005 and R0402 are selected and soldered using SAC305 (Sn3.0Ag0.5Cu). The investigation of thermal fatigue life of inconsistently shaped solder joints is carried out experimentally by continuous thermal shock loading. In the numerical approach, finite element analysis is conducted to calculate accumulated inelastic strain energy density. Moreover, Darveaux's model constants for chip resistor assembly are obtained using experimental lifetime and numerically acquired accumulated inelastic strain energy density.

2 Experimental Methodology

In surface mount technology, the final shape of the solder joint is determined by natural processes that minimize the accumulated energy from various factors such as surface tension, gravity, hydrostatic, and capillary pressure as the molten solder solidifies, based on the given dimensions of component and pads [15–17]. Moreover, the molten solder takes different shapes depending on the solder volume. The solder volume is usually controlled by the aperture on a stencil. However, it is highly dependent on the design parameter of the aperture such as aperture shape, stencil thickness, corner ratio, and surface roughness [18,19]. Therefore, there is a challenge in accurately depositing the desired solder volume during the printing solder paste process. Manufacturers use their own criteria to determine whether solder joints pass or fail, which can vary depending on the assembly house and maker. Within the pass range, the chip resistors are all considered to have passed regardless amount of solder paste. This means that there may be a discrepancy between the designed solder volume and the actual solder volume deposited. As a result, molten solder can solidify into different shapes, resulting in a single resistor being interconnected with two differently shaped solder joints. This differently shaped solder joint is closely associated with thermal fatigue life.

2.1 Prediction of Solder Joint Shape in Surface Evolver. To analyze the effect of nonsymmetrical solder shape in a single resistor on fatigue life, Surface Evolver is utilized to predict the final solder joint shape with the given geometry of component and pads [20]. The 3D model using Surface Evolver is created as shown in Fig. 1, using input parameters in the model, as listed in Table 1. The material properties of SAC305 are also included as input parameters in the model as shown in Table 2. The chip resistor in the model featured a rectangular ceramic body and three faces of termination on each end, which are colored deep red. The pastes are applied boundary conditions to prevent overspreading and ensure that they stay within only the pads and terminations.

The solder shapes under different solder volumes in the model are compared with the samples' cross section to validate the model as shown in Fig. 2. As studied in many researches, standoff height in solder joint is one of major factors, which is closely related to the fatigue life [11,12]. During thermal cycling, the crack generally

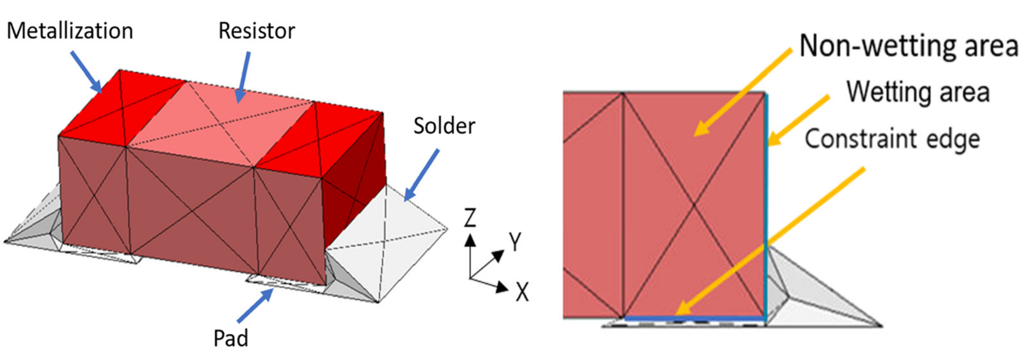

Fig. 1 Chip resistor assembly in Surface Evolver

Table 1 Specs of component and pad

Item	R0402 (mm)	R1005 (mm)
Component (L × W × H)	0.40 × 0.20 × 0.15	1.0 × 0.50 × 0.35
Termination length	0.13	0.23
Copper pad (L × W)	0.20 × 0.22	0.50 × 0.56
Pad gap	0.16	0.46

Table 2 Material properties of SAC305

Solder	Contact angle	Surface tension [21]	Density
SAC305	24 deg	544.9 dyne/cm	7.361 g/cm^3

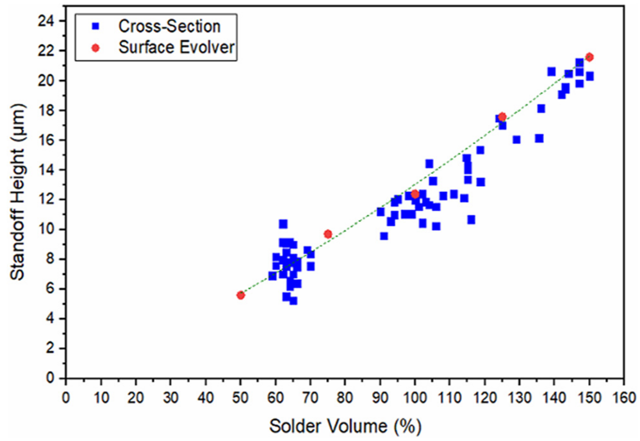

Fig. 3 Surface Evolver model and sample standoff height comparison

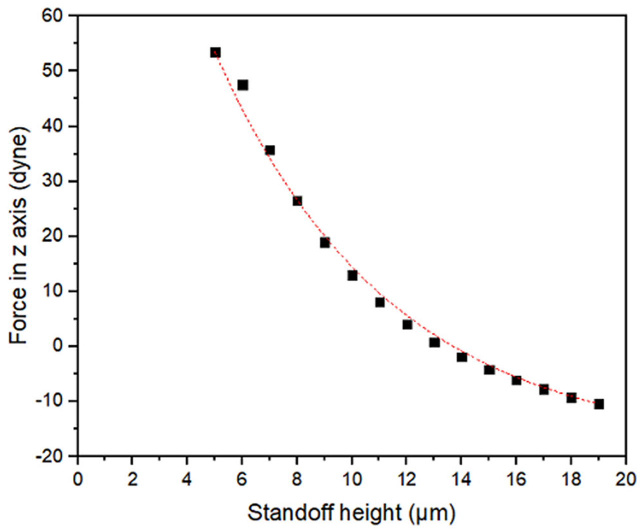

Fig. 4 Force in *z* axis with respect to height

tends to initiate in the underneath of solder joint due to the CTE mismatch between the chip resistor and pad. The molten solders change their shapes by minimization of energy during reflow. Meantime, the chip resistor is adjusted its position by the molten solders to maintain to equilibrium state. In order to investigate underneath of solder joint, the chip resistor model in Surface Evolver is built up to move the position freely in resistor's length, width and height directions with change of solder joint shapes. Thus, the chip resistor in Surface Evolver would be positioned in different heights by molten solder with respect to different solder volumes.

Various standoff height can be predicted with respect to the solder volumes and compared with samples as shown in Fig. 3. Figure 4 represents force calculation in z-axis with respect to different standoff heights when 100% solder volume is applied in the model.

Then, volumes of solder pastes required to induce the predetermined solder shapes, concave, straight, tiny convex, and convex, are found in the model. The solder pastes volumes of 0.0018406 mm^3 for R0402 and 0.027712 mm^3 for R1005 are used as a reference 100% for straight shape solder joint. The difference in solder paste volume between each shape is set at 40%. The resulting predetermined solder shapes are visualized in Fig. 5, while the corresponding solder volumes for each shape can be found in Table 3.

Optimizing stencil apertures are crucial to deposit solder paste effectively since all chip resistors having different solder shapes in the board share the same stencil. Laser cutting fabrication is commonly used due to its cost-effectiveness. However, electroforming is used to fabricate the stencil to consider the largest solder volume, which is a convex shape for R1005, and the smallest solder volume, which is a concave shape for R0402 with a minimum thickness of stencil. The thickness of the stencil is decided as 0.07112 mm to avoid bridging and insufficient deposition. Rectangular apertures with rounded corners are designed for concave, straight, tiny convex, and convex shapes to accommodate the required solder paste volume. Additionally, two different apertures are selected and integrated into a single chip resistor to make eight pairs of apertures. Thus, eight pairs of differently shaped

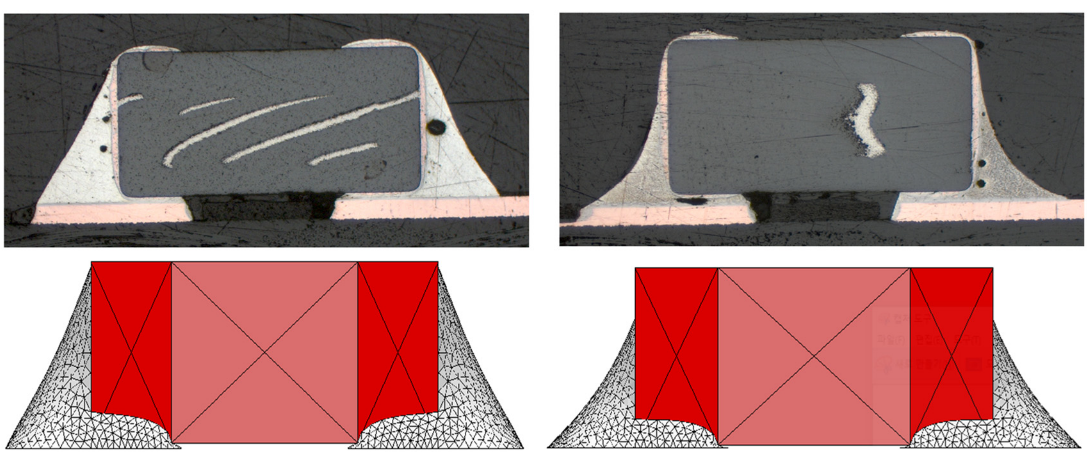

Fig. 2 Comparison of model in Surface Evolver and samples' cross section: (*a*) 101–104% and (*b*) 66–65% solder volumes

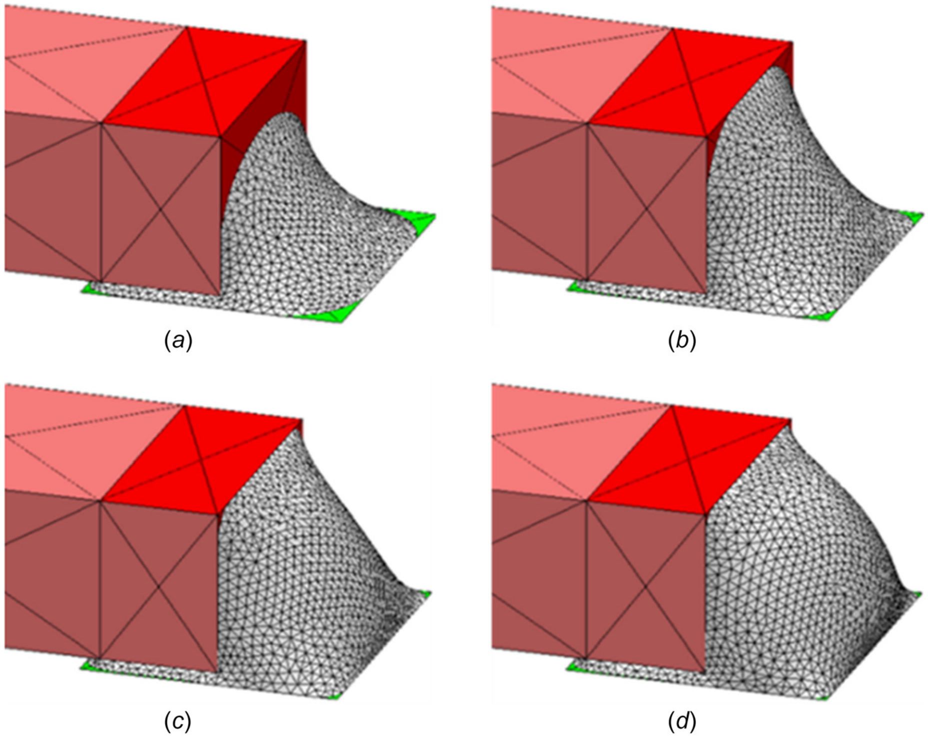

Fig. 5 Redetermined solder shapes in Surface Evolver: (*a*) concave, (*b*) straight, (*c*) tiny convex, and (*d*) convex

Table 3 Solder volumes of predetermined shapes

Component type	Solder shape	Volume (%)
R0402	Concave	60
	Straight	100
R1005	Tiny convex	140
	Convex	180

solder joints of chip resistors are assembled. Figure 6 shows the eight pairs of apertures used to assemble nonsymmetric solder joints on a single chip resistor, and Fig. 7 shows the stencil layout. Solder pastes on pads are inspected to ensure the deposition properly as shown in Fig. 8.

2.2 Test Board Configuration. The FR-4 PCB is sized of 265 × 215 × 16 mm, and there are two types of rectangular chip resistor, R1005 (1.0 × 0.5 × 0.35 mm) and R0402 (0.4 × 0.2 × 0.15 mm), tin finish on nickel, mounted with SAC305 (Sn3.0Ag0.5Cu) on the electroless nickel immersion gold through reflow process. The reflow profile is optimized to ensure that solder paste melts completely and then forms robust joints [22–24] as shown in Fig. 9.

The experiment is designed that different volumes of solder paste are deposited on the PCB, which form differently shaped solder joints. Specifically, the PCB is arranged so that two different shapes of solder joints are used to secure each resistor in place. The chip resistors of the first two columns on PCB use symmetrical solder shapes, such as concave–concave and straight–straight, while the remaining use nonsymmetrical solder shape. The PCB layout and the number of columns are shown in Fig. 10, and Table 4 represents the solder shape conditions corresponding to the column in PCB. Using Surface Evolver model, solder joint shapes are predicted depending on the solder paste deposition after reflow process as shown in Fig. 11.

To perform the fatigue life test in a harsh environment such as aerospace or automotive applications, extremely harsh thermal shock cycling is employed. The experiment adopts the temperature cycling from −55 °C to 150 °C with 3 min of dwell time and 2 min of ramp time based on the standards, JESD22-A106 and IEC-60068 as shown in Fig. 12 [25,26].

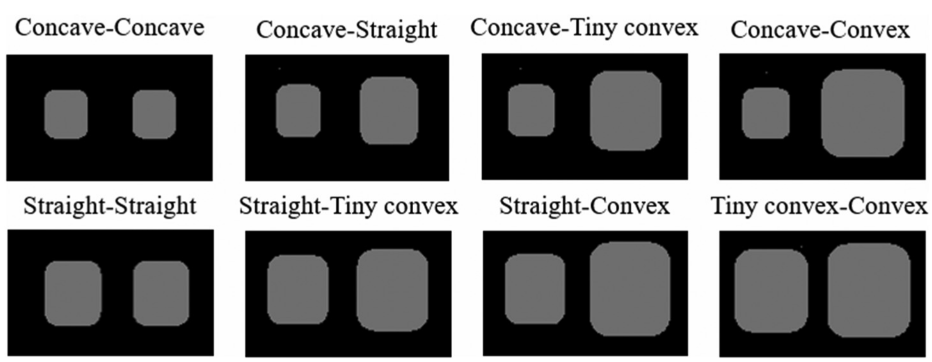

Fig. 6 Eight pairs of stencil aperture designs

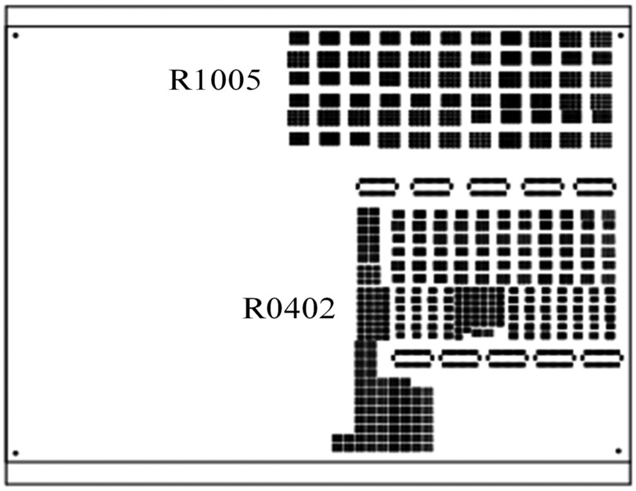

Fig. 7 Stencil layout

The test board contains eight columns for each type of chip resistor, and each of eight columns features a different set of solder shapes. Each column consists of six groups, and 20 chip resistors are connected together in a daisy-chain configuration to form one group. The setup enables the in situ monitoring of resistance changes in each group via a single channel of a connector as depicted in Figs. 13(*a*) and 14.

Previously, researchers have investigated failures by using different criteria such as a 20% increase in resistance, a resistance threshold, or an infinite resistance. The change in resistance during a failure of a solder joint can be categorized into three stages, stable, crack, and open, with the resistance changing significantly depending on the stage. In the stable stage, no crack starts, or the crack is very small, resulting in a stable resistance value. In the crack stage, the crack could propagate enough to cause a change in resistance, while in the open stage, the crack is fully occurred and electrically disconnected, resulting in an infinite resistance value. Therefore, the definition of a failure of a solder joint would vary depending on the criteria. The precise value of resistance change that indicates a failure is not clear, and different researchers have reported different failure criteria as resistance threshold of 50Ω, 100Ω, or a percentage increase in resistance of 10% or 20%. The time to failure also varies based on the failure criterion chosen [27,28]. In this experiment, the infinite value of resistance, which is hard open, is adopted as the failure criterion because of the relatively large initial value of resistance, which may make it difficult to detect small resistance changes caused by a small crack. Additionally, there is also the possibility of an error caused by electrical noise in the cable damaged by exposure to constant temperature changes. In the event of a failure, the samples are examined microscopically after being cross-sectioned to identify the failure mechanism caused by thermal shock cycling.

Table 4 Details of solder shape variations in board

Number	Component	Solder shape	Condition
1	R1005	Concave–concave	Symmetric
2		Concave–straight	Nonsymmetry
3		Concave–tiny convex	
4		Concave–convex	
5		Straight–straight	Symmetry
6		Straight–tiny convex	Nonsymmetry
7		Straight–convex	
8		Tiny convex–convex	
9	R0402	Concave–concave	Symmetric
10		Concave–straight	Nonsymmetry
11		Concave–tiny convex	
12		Concave–convex	
13		Straight–straight	Symmetry
14		Straight–tiny convex	Nonsymmetry
15		Straight–convex	
16		Tiny convex–convex	

Zone	1	2	3	4	5	6
Programmed Temperature (ºC)	100	140	155	170	240	270

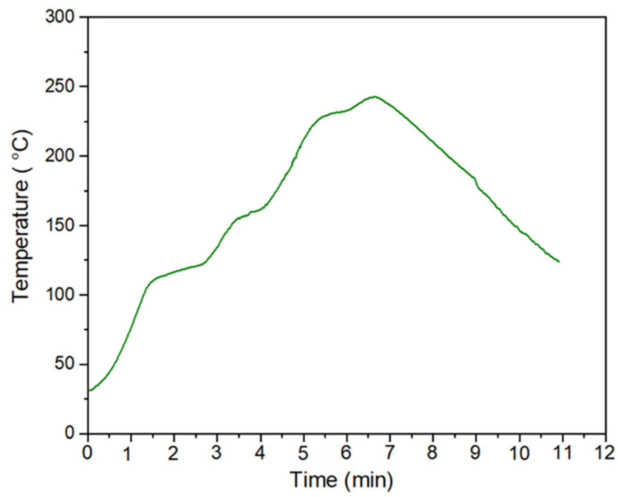

Fig. 9 Programed and measured reflow profile

3 Results and Discussions

3.1 Fatigue Life Experiment Results. The Weibull plots in Figs. 15(*a*) and 15(*b*) depict the results of thermal shock test performed on differently shaped solder joints for R1005, while Figs. 15(*c*) and 15(*d*) display the corresponding results for R0402. The most reliable solder joint in terms of thermal shock, as shown in Fig. 15(*a*), is a symmetrically shaped solder joint on both ends of a single resistor, which has a characteristic time to failure (TTF. 63.2%) of 10,873 cycles. Following this, concave–straight shape

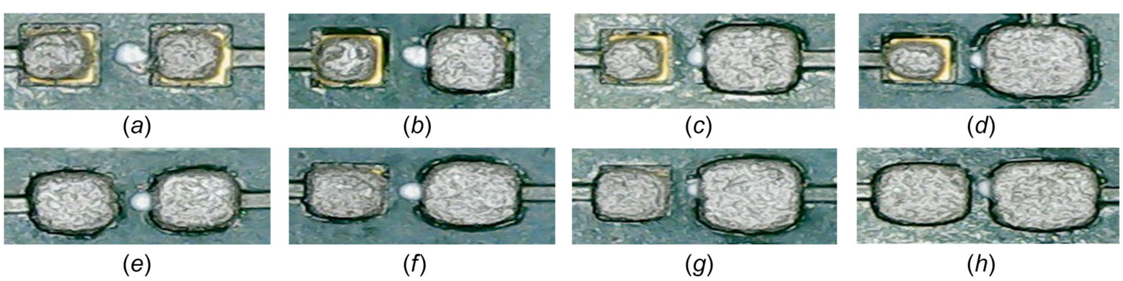

Fig. 8 Printed solder pastes: (*a*) concave-concave, (*b*) concave-straight, (*c*) concave-tiny convex, (*d*) concave-convex, (*e*) straight-straight, (*f*) straight-convex, and (*h*) tiny convex-convex

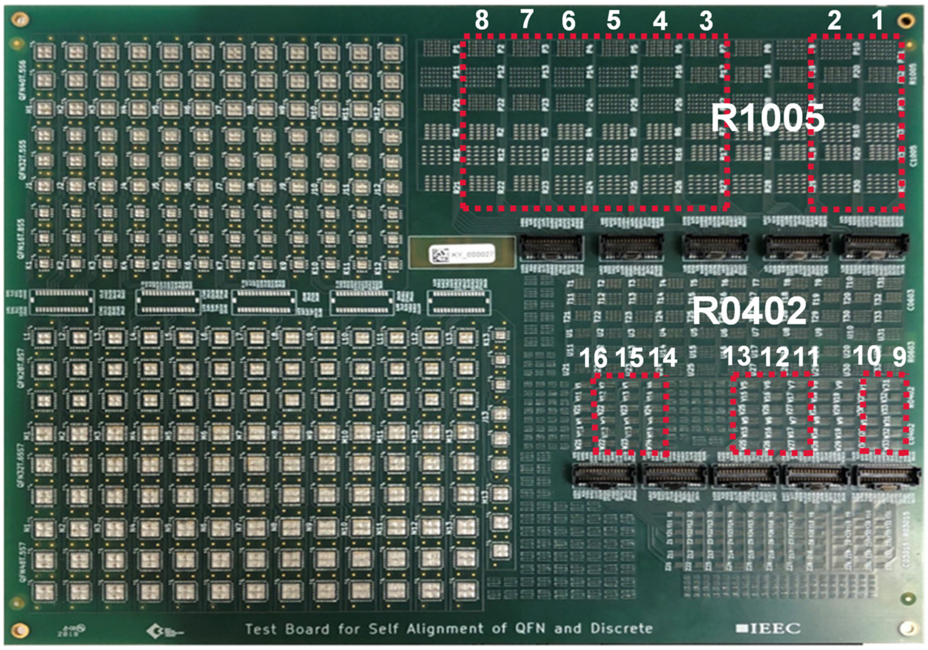

Fig. 10 PCB layout and elements number

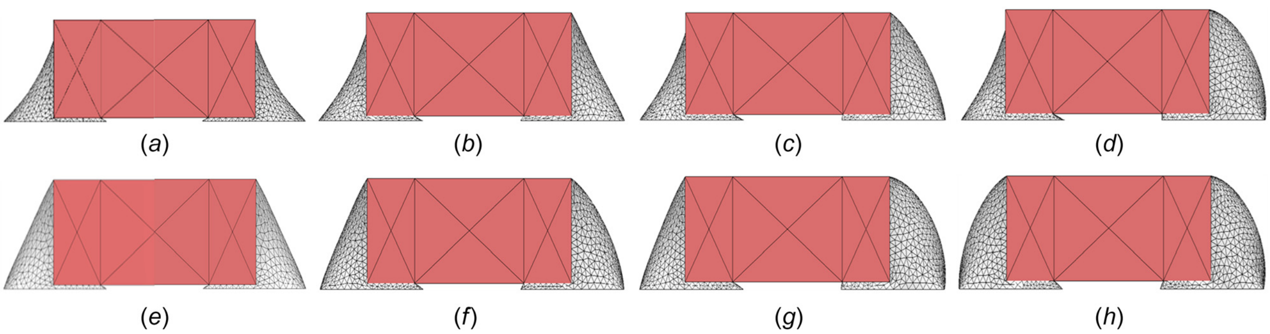

Fig. 11 Variations of non-(*a*) concave-concave, (*b*) concave-straight, (*c*) concave-tiny convex, (*d*) concave-convex, (*e*) straight-straight, (*f*) straight-tiny convex, (*g*) straight-convex, and (*h*) tiny convex-convex

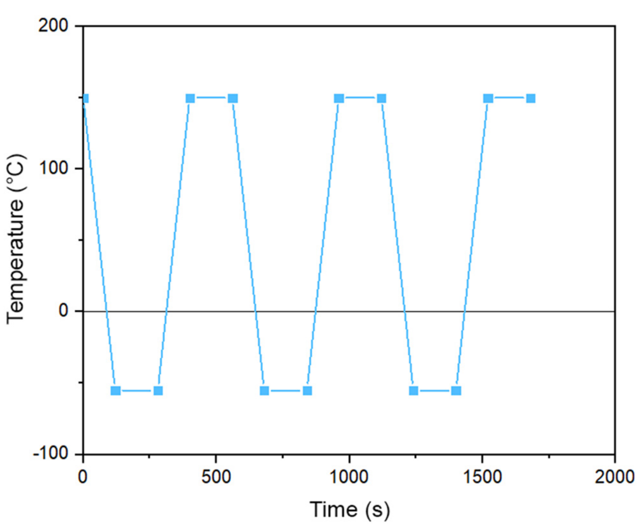

Fig. 12 Thermal shock cycling profile

comes in next with a TTF of 10,577 cycles, while concave–tiny convex shape has a TTF of 10,131 cycles. Concave–convex shape shows the lowest thermal shock resistance with TTF of 9874 cycles.

As shown in Fig. 15(*b*), Weibull plot for a straight shaped solder joint on one pad side, straight–straight, which is a symmetrically shaped solder joint, is found to be the most thermal shock reliable with TTF of 11,737 cycles. Straight–tiny convex is the second with a TTF of 11,153 cycles, while straight-convex shape shows the most failures with a TTF of 10,359 cycles. Moreover, the tiny convex–convex shape exhibits the most reliability against thermal shock cycling with TTF of 13,836 cycles among the nonsymmetrically shaped solder joints of a single resistor. According to the results, chip resistor assemblies, which have symmetrically shaped solder joints on two pads, has better thermal shock resistance compared to assemblies with differently shaped solder joints. Furthermore, a larger difference in solder volume between two pads leads to earlier solder joint failures. Figure 16 depicts the results of experiments, in which solder volume differences of 40% and 80% with different total amounts of solder volumes on two pads to observe changes in fatigue life. The plots indicate that increasing the total amount of solder volume on the two pads improves the reliability of the chip resistor assembly, even when the solder volume difference between two pads is the same, as seen in the

Table 5 TTF of variations of solder shape

Component	Solder shape	TTF 63.2%	% difference
R1005	Concave–concave	10,873	
	Concave–straight	10,577	2.76
	Concave–tiny convex	10,131	7.07
	Concave–convex	9874	9.63
	Straight–straight	11,737	
	Straight–tiny convex	11,153	5.10
	Straight–convex	10,359	12.47
	Tiny convex–convex	13,836	
R0402	Concave–concave	12,727	
	Concave–ctraight	11,814	7.44
	Concave–tiny convex	11,425	10.78
	Concave–convex	11,066	13.96
	Straight–straight	13,508	
	Straight–tiny convex	12,794	5.43
	Straight–convex	12,318	9.22
	Tiny convex–convex	15,612	

comparison between concave–straight and straight–tiny convex shapes.

During repeated thermal shock cycling, the chip resistor with solder joints and PCB experience expansion and contraction, and extremely harsh temperature cycling will generate larger expansion and contraction. As a result, more stress caused by CTE mismatch will be generated on the smaller volume of solder joints, and a crack also propagates more rapidly along the fillet on the solder joint in Fig. 17. The smaller resistor, R0402 exhibits a longer fatigue life than the larger resistor, R1005 because of lesser stress generated during chip resistor contraction (Table 5).

3.2 Life Prediction Model. Based on the experimental results, the fatigue life prediction of SAC305 solder joint becomes possible through the Anand Model, which is commonly used to represent the nonlinear behavior of solder material [29]

$$\frac{d\varepsilon_p}{dt} = A[\sinh(\xi\sigma/s)]^{1/m}\exp\left(\frac{-Q}{\mathrm{kT}}\right) \quad (1)$$

$$\frac{ds}{dt} = \left\{h_0(|B|)^a \frac{B}{|B|}\right\}\frac{d\varepsilon_p}{dt} \quad (2)$$

$$B = 1 - \frac{s}{s^*} \quad (3)$$

$$s^* = \hat{s}\frac{d\varepsilon_p/dt}{A}\exp\left(\frac{Q}{\mathrm{kT}}\right)^n \quad (4)$$

According to the constants in the constitutive equation as shown in Table 6, a finite element model is utilized to predict the fatigue life of SAC305 based on the inelastic strain energy density accumulated per each cycle of solder joints. The finite element analysis (FEA) model is comprised of a chip resistor, PCB, pad, solder mask, and SAC305 solder joints. The geometry of solder joint is imported from the Surface Evolver model to build more realistic shapes as shown in Fig. 18 and dimensions and propeties present in Tables 7 and 8. Due to simplification of analysis, the half symmetry model is employed, and material properties in the model are applied as linear elastic solid expect solder joints as nonlinear. Element type of solid 186, which is higher order quadratic element, is selected for chip resistor, PCB, and solder mask while solid 187 and 186 are for pad, termination, and solder joint due to complicated geometry for meshing.

To predict the fatigue life in the fatigue life in the chip resistor assembly, two-steps simulation is used. In the first step, the entire model undergoes thermal shock cycling to determine the average plastic work of the underneath in the solder joint, which is the area between the chip resistor and pad. Subsequently, in the second step, the model excluding the underneath, which is already calculated in the first step, is rerun to calculate the plastic work on the fillet of the solder joint. The fillet geometry on solder joint is split into three possible crack paths: 0 deg, 45 deg, and 90 deg, and the highest plastic work, which induces the lowest fatigue life among the possible crack paths, is determined as shown in Fig. 19. The reason for dividing into two steps is that a crack commonly initiates in the underneath of solder joint and propagates along the fillet of the solder joint. Then the crack will emerge on the surface of the solder joint. Once the crack begins propagating along the fillet, the underneath of solder joint is electrically disconnected fully from the pad and chip resistor so that is assumed that the underneath of the solder joint cannot play a role.

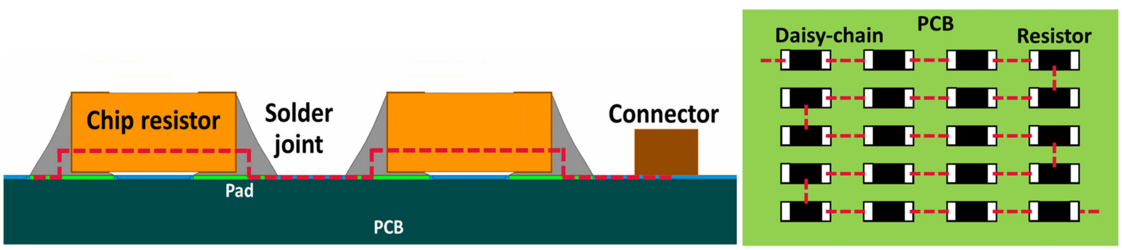

Fig. 13 Daisy-chain structure

Fig. 14 Experiment setup for in situ measurement of resistance change

In finite element analysis, the mesh density strongly influences on the results as known as mesh sensitivity. The plastic energy density values to calculate the fatigue life may vary depending on the mesh quality in this study. To achieve near mesh-independent results and reasonable analysis time, it is necessary to identify the suitable mesh density. Three distinct mesh size models are generated and compared the results and analysis times as shown in Table 9. It is shown that the differences in accumulated energy density between

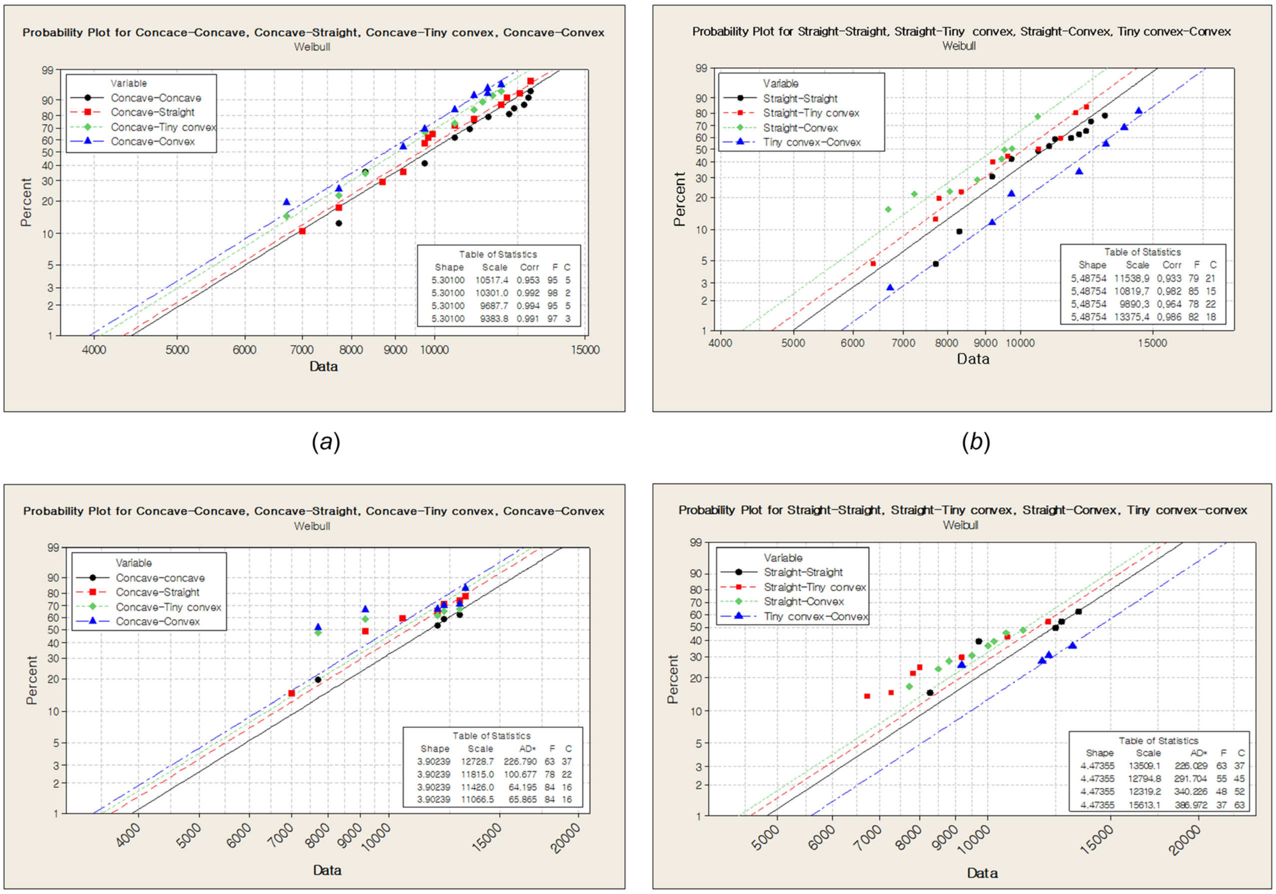

(*a*) (*b*)

(*c*) (*d*)

Fig. 15 Weibull plot of thermal shock cycling result of nonsymmetrical shape for (*a*) concave shape solder joint on one pad side of R1005, (*b*) straight shape solder joint of on one pad of R1005, (*c*) concave shape solder joint on one pad side of R0402, and (*d*) straight shape solder joint of on one pad of R0402. (*a*) Probability plot for concace–concave, concave–straight, concave–tiny convex, concave–convex Weibull, (*b*) probability plot for straight–straight, straight–tiny convex, straight–convex, tiny convex–convex Weibull, (*c*) probability plot for concave–concave, concave–straight, concave–tiny convex, concave–convex Weibull, and (*d*) probability plot for straight–straight, straight–tiny convex, straight–convex, tiny convex–convex Weibull.

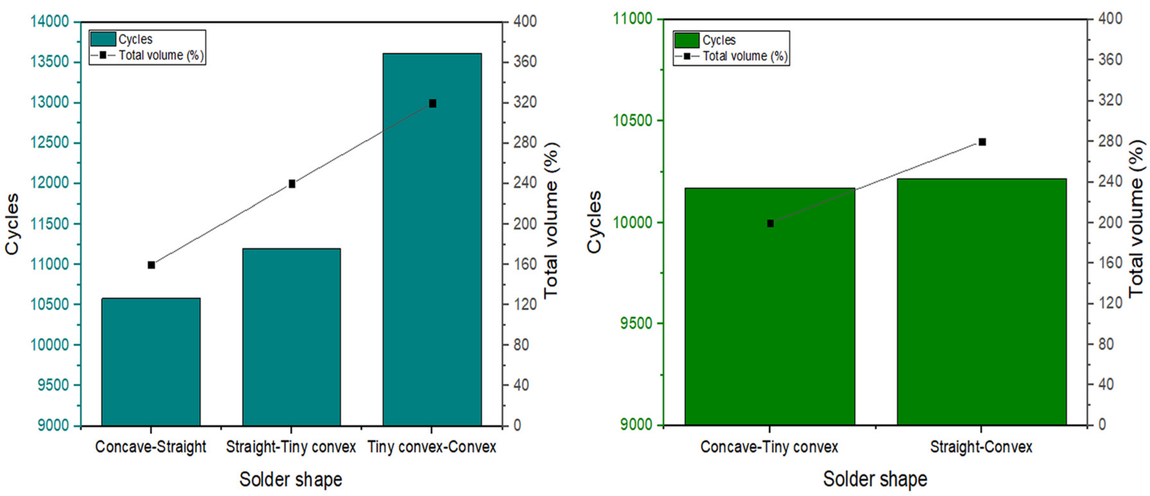

(*a*) (*b*)

Fig. 16 TTF 63.2% plots: (*a*) 40% of volume difference and (*b*) 80% of volume difference on two pad sides of a single resistor

Table 6 Constants of Anand model for SAC305

Parameter	Definition	Value
s_0 (MPa)	Initial value of deformation resistance	2.15
Q/k (K)	Activation energy of solder/Boltzmann's constant	9970
A $(1/s)$	Pre-exponential factor	17.994
Ξ	Multiplier of stress	0.35
m	Strain rate sensitivity of stress	0.153
h_0 (MPa)	Hardening constant	1526
$\hat{s}$	Coefficient for deformation resistance saturation value	2.536
n	Strain rate sensitivity of saturation value	0.028
a	Strain rate sensitivity of hardening	1.69

Table 7 Assembly dimensions in FEA model

Materials	Dimensions (mm)
Termination thickness	0.007
Copper pad	0.56 × 0.5 × 0.02
Solder mask thickness	0.02
PCB	3.42 × 2.56 × 1.58

Table 8 Material properties in FEA model

Materials	Young's modulus (GPa)	Poisson's ratio	CTE (ppm/°C)
Resistor	282.7	0.22	6.67
Termination	83	0.37	18.9
Solder	28–48	0.40	21.7
Copper pad	121	0.34	16.7
PCB	16.5–21.5	0.39	16.5
Solder mask	2.4	0.30	60–160

Table 9 Results of different mesh models

		Mesh 1	Mesh 2	Mesh 3
Mesh size (μm)		20	10	5
Acc. energy density (MPa)	Underneath	0.38654	0.38036	0.36922
	Fillet	0.49726	0.48902	0.47404
% Diff in acc. energy density	Underneath		1.60	2.93
	Fillet		1.85	3.06
% Diff. in time	Underneath		58	57
	Fillet		22	29

three models are less than 5% while analysis time of mesh 3 model is slightly higher than other models. Hence, mesh 2 model is selected for this study to perform with efficient computing resources.

Darveaux's model is widely adopted to calculate the fatigue life based on inelastic strain energy density accumulated per thermal cycle among many other models such as Steinburg's stress based [30] and Engelmaier's strain based [31] models

$$N_0 = K_1 \cdot \Delta W_{\text{avg}}^{K_2} \tag{5}$$

$$\frac{da}{dN} = K_3 \cdot \Delta W_{\text{avg}}^{K_4} \tag{6}$$

$$\alpha = N_0 + \frac{a}{da/dN} \tag{7}$$

where N_0 is the number of cycles crack initiated which is usually negligible, da/dN is crack propagation rate, a is crack length, ΔW_{avg} is accumulated energy density, K_1, K_2, K_3, and K_4 are fatigue model constants, and α is total fatigue life. The K values can be experimentally and numerically obtained, and they are defined based on the geometry of the solder joints and the size of the package [32,33]. In this study, crack initiation cycle, N_0 is not considered to calculate the total fatigue life for the solder joints in chip resistor due to relatively smaller number, which is approximately less than 10% of total life cycles [33–35].

The results of life prediction models for differently shaped solder joints on a single resistor are presented in Table 10. The plastic works and calculated cycles of both solder joints on two pads are compared and the solder joint, which has a smaller lifetime, would be selected to compare with experimental results. As compare the fatigue life of underneath solder joints, the fatigue life of smaller volume of solder joint increases while fatigue life of larger volume of solder joint decreases. However, the fatigue life of fillet on smaller solder volume joints rapidly decrease as volume difference between two pads is going bigger. Thus, the smaller volume of solder joint between solder joints on two pads has the shortest reliability and failures earlier than the solder joint which deposited larger solder volume side. The volume difference between two solder joints affects the final positions of the chip resistor. As the difference increases, the chip resistor shifts toward to the smaller volume of solder joint during reflow because of the self-alignment characteristic of surface mount assemblies [36,37]. In that manner, a chip resistor becomes sufficiently mispositioned to shorten the fatigue life and it tends to be higher as volume difference between two solder joints increases. Nevertheless, the effect of the volume difference between two solder joints on fatigue life shrinks as the

Table 10 Results of fatigue life prediction models

			ΔW_{avg} (MPa)		Crack length (μm)		Life cycle			
Sample	Conditions	Solder shape	Underneath	Fillet	Underneath	Fillet	Underneath	Fillet	Total cycle	% difference
A	Concave–concave	Concave	0.39059	0.41405	240	264	5190	5506	10,696	
B	Concave–straight	Concave	0.40437	0.44250	242	274	5112	5490	10,602	0.88
		Straight	0.43748	0.43991	234	351	4717	7053	11,771	
C	Concave–tiny convex	Concave	0.41071	0.49786	235	280	4924	5210	10,134	5.40
		Tiny convex	0.45417	0.49062	230	358	4531	6727	11,257	
D	Concave–convex	Concave	0.38051	0.59970	283	364	5362	4690	10,052	6.21
		Convex	0.41170	0.44385	228	364	4762	7278	12,040	
E	Straight–straight	Straight	0.38036	0.48902	240	347	5276	6530	11,806	
F	Straight–tiny convex	Straight	0.38021	0.56680	247	355	5425	6104	11,528	2.38
		Tiny convex	0.39706	0.47284	234	361	5009	6943	11,952	
G	Straight–convex	Straight	0.35478	0.76543	244	358	5599	5105	10,704	9.80
		Convex	0.37993	0.49966	228	368	5004	6839	11,843	
H	Tiny convex–convex	Tiny convex	0.29635	0.43078	246	372	6303	7264	13,567	
		Convex	0.29792	0.33911	236	374	6041	8815	14,856	

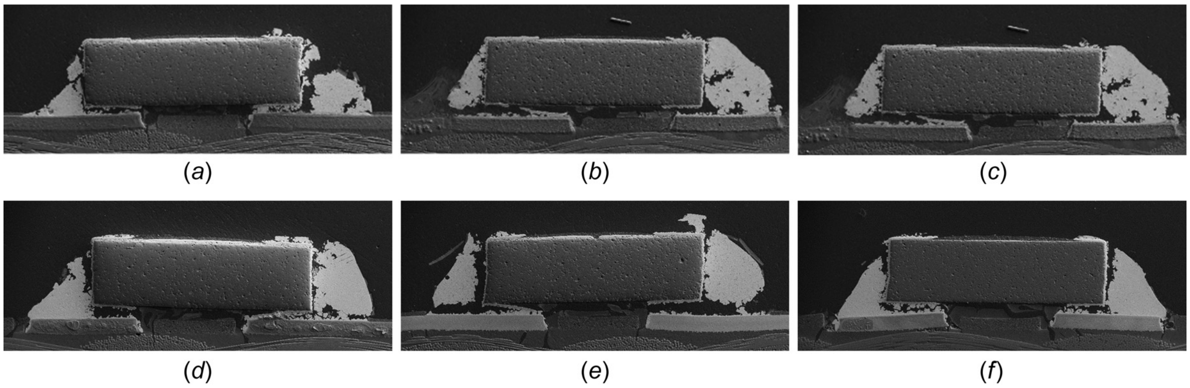

Fig. 17 SAC305 solder joint images representative thermal shock fatigue failures: (*a*) concave–straight, (*b*) concave–tiny convex, (*c*) concave–convex, (*d*) straight–tiny convex, (*e*) straight–convex, and (*f*) tiny convex–convex

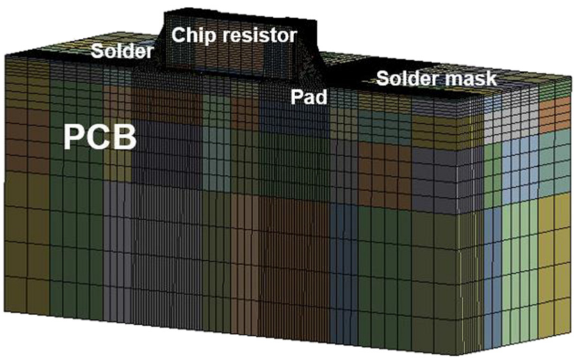

Fig. 18 Half symmetry FEA model

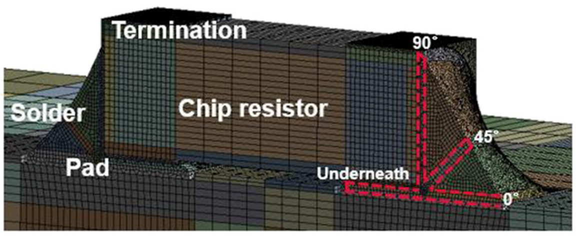

Fig. 19 Possible crack paths on solder joint

total volume of two solder joints increases. As shown in Fig. 16 and Table 10, samples B, F, and H have 40% of solder volume difference between two joints, but the results show that fatigue life is increased in the order of samples B, F, and H. Therefore, larger solder deposits on two pads offer increased reliability even though their volume difference between two joints is the same. The model reveals the potential time to failure of electrical connection of a chip resistor is determined by the smaller solder joint side.

Since crack initiation cycles is not taken into account, the values of constants, K_3 and K_4 are obtained by plugging the lifetime, accumulated energy density, and crack length acquired experimentally and numerically into Eq. (8). The constant values are presented in Table 11

Table 11 Darveaux's model constant

Constant	K_3 $(\mu\text{m/cycle}\cdot\text{MPa}^{K_4})$	K_4
Value	0.0827	0.6183

Table 12 Comparison of experimental data and finite element prediction

Solder shape	Experimental N_f	FEA N_f	% Difference
Concave–concave	10,873	10,696	4.65
Concave–straight	10,577	10,602	0.23
Concave–tiny convex	10,131	10,134	0.03
Concave–convex	9874	10,052	1.79
Straight–straight	11,737	11,806	0.58
Straight–tiny convex	11,153	11,528	3.25
Straight–convex	10,359	10,704	3.22
Tiny convex–convex	13,836	13,567	1.96

$$\alpha_{\text{total}} = \alpha_{\text{underneath}} + \alpha_{\text{fillet}} = \frac{a_1}{K_3\cdot\Delta W_{\text{avg1}}^{K_4}} + \frac{a_2}{K_3\cdot\Delta W_{\text{avg2}}^{K_4}} \tag{8}$$

where a_1 and a_2 are the crack length of underneath and fillet in solder joint and $\Delta W_{\text{avg},1}$ and $\Delta W_{\text{avg},2}$ are the accumulated energy density in underneath and fillet in solder joint. The results of the experiment and life prediction model are presented and compared in Table 12. The results are in good agreement with the experimental data.

4 Conclusions

The purpose of this study is to present an optimized solder volume with respect to solder shape which extends thermal reliability through comparing fatigue life of different solder volumes. Assembly house and makers utilize their own pass/fail criterion on the solder paste volume to assembly electronics. Regarding it, a single chip resistor run the risk of being connected two differently shaped solder joints. Moreover, variations of differently shaped solder joints on a chip resistor assembly induce variations in reliability. In this paper, thermal reliability of various nonsymmetric solder joints that are commonly adopted/accepted? In assembly house and makers was experimentally and numerically evaluated. The result from this study is found that difference of solder joint volumes between two pads on a single chip resistor highly influences on the fatigue life and total amount of solder volume deposited on two pads is also one of major factor affecting the reliability. Furthermore, a new set of Darveaux's model constants is established using data obtained experimentally and numerically for this typical assembly. It allows that the fatigue life of various solder joint shape is predicted in finite element analysis for SAC305 in chip resistor assembly.

This study used Surface Evolver to create three-dimensional models, which have four predetermined solder shapes: concave, straight, tiny convex, and convex. A uniquely designed stencil is manufactured to have various apertures depositing the solder pastes generating predetermined solder shapes. Eight pairs of solder joints are assembled to hold a chip resistor in place so that reliability of differently shaped solder joint on a single chip resistor could be compared under the thermal shock cycling (−55 °C to 150 °C with 3 min of dwell time and 2 min of ramp time). Two types of chip resistors, R1005 ($1.0 \times 0.5 \times 0.35\,mm^3$) and R0402 ($0.4 \times 0.2 \times 0.15\,mm^3$) are mounted with SAC35 (Sn3.0Ag0.5Cu) on the electroless nickel immersion gold pads. Based on the results of a fatigue life test, the symmetrically shaped solder joints, which is concave–concave shape of solder joint show the best thermal shock resistance, differently shaped solder joints, which is concave–straight the second, concave–tiny convex the fourth, and concave–convex has the shortest fatigue life among the assemblies which had the concave shape on one pad side. Moreover, straight–straight shape indicates the most reliability, straight–tiny convex the second, and straight–convex shows the most failures. Overall, the fatigue life is decreased if the volume difference between two solder joints increases. However, the fatigue life is increased as the total sum of solder volume of two solder joints is increased even though the volume difference between two joints keeps the same. Thus, the fatigue life of differently shaped solder joints is dominated by the smaller volume solder joint.

Based on the results, this study has made contributions in identifying the impact of solder volume variations on the formation of solder shapes during reflow and their fatigue life. This study provides the guidelines to determine proper solder volumes in chip resistor assembly in order to obtain desired fatigue life. These findings and coefficients enhance the understanding of the thermal shock reliability of differently shaped SAC305 solder joints on a single chip resistor, providing guideline to assembly house and makers improving the overall performance and longevity of surface mount components.

Data Availability Statement

The authors attest that all data for this study are included in the paper.

Nomenclature

a = crack length
a = strain rate sensitivity of hardening
A = pre-exponential factor
h_0 = hardening constant
k = gas constant
K_i = Darveaux's model constants
m = strain rate sensitivity of stress
n = strain rate sensitivity for saturation value of deformation resistance
N_0 = crack initiation cycles
Q = activation energy
s = internal state variable, deformation resistance
s^* = saturation value of deformation resistance
$\hat{s}$ = coefficient of saturation value of deformation resistance
T = absolute temperature
α = total fatigue life
ΔW_{avg} = accumulated inelastic strain energy density
ξ = multiplier of stress
σ = equivalent stress
$\frac{da}{dN}$ = crack propagation rate
$\frac{ds}{dt}$ = evolution equation
$\frac{d\varepsilon_p}{dt}$ = inelastic strain rate

References

[1] Ha, J., Cai, C., Yin, P., Lai, Y., Pan, K., Yang, J., and Park, S., 2022, "Shape Dependency of Fatigue Life in Solder Joints of Chip Resistors," 72nd Electronic Components and Technology Conference (ECTC), San Diego, CA, May 31–June 3, pp. 1489–1494.
[2] Yin, P., Park, S., Jacob, B., Yin, L., and Gowda, A., 2022, "Package Design Through Reliable Predictive Modeling and Its Validation," 72nd Electronic Components and Technology Conference (ECTC), San Diego, CA, May 31–June 3, pp. 1738–1744.
[3] Klein Wassink, R. J., and Verguld, M. M. F., 1986, "Drawbridging of Leadless Components," Microelectron. Int., **3**(1), pp. 18–24.
[4] Ellis, J. R., and Masada, G. Y., 1990, "Dynamic Behavior of SMT Chip Capacitors During Solder Reflow," IEEE Trans. Compon., Hybrids, Manuf. Technol., **13**(3), pp. 545–552.
[5] Krammer, O., 2014, "Modelling the Self-Alignment of Passive Chip Components During Reflow Soldering," Microelectron. Reliab., **54**(2), pp. 457–463.
[6] Heinrich, S. M., Liedtke, P. E., Nigro, N. J., Elkouh, A. F., and Lee, P. S., 1993, "Effect of Chip and Pad Geometry on Solder Joint Formation in SMT," ASME J. Electron. Packag., **115**(4), pp. 433–439.
[7] Goldmann, L. S., 1969, "Geometric Optimization of Controlled Collapse Interconnections," IBM J. Res. Develop., **13**(3), pp. 251–265.
[8] Lu, H., Bailey, C., Dusek, M., Hunt, C., and Nottay, J., 2000, "Modelling the Fatigue Life of Solder Joints for Surface Mount Resistors," International Symposium on Electronic Materials and Packaging (EMAP2000), Hong Kong, China, Nov. 30–Dec. 2, pp. 136–142.
[9] Pan, K., Ha, J. H., Wang, H., Xu, J., and Park, S., 2021, "An Analysis of Solder Joint Formation and Self-Alignment of Chip Capacitors," IEEE Trans. Compon., Packag., Manuf. Technol., **11**(1), pp. 161–168.
[10] Ha, J., Pan, K., Wang, H., Won, D. H., and Park, S. B., 2020, "The Effect of Misaligned Passive Component on Fatigue Life of Solder Joints and Solder Shape," 19th IEEE Intersociety Conference on Thermal and Thermomechanical Phenomena in Electronic Systems (ITherm), Orlando, FL, July 21–23, pp. 1029–1034.
[11] Garami, T., and Krammer, O., 2013, "Investigating the Mechanical Effect of the Solder Joint Thickness With Simulation," 19th International Symposium for Design and Technology in Electronic Packaging (SIITME), Galati, Romania, Oct. 24–27, pp. 259–262.
[12] Wang, H., Pan, K., Ha, J., Cai, C., Xu, J., and Park, S., 2019, "The Effect of Solder Paste Volume on Chip Resistor Solder Joint Fatigue Life," Procedia Manuf., **38**, pp. 1372–1380.
[13] Mohamed Sunar, M. S., Abu Bakar, M., Jalar, A., Ramli, M. R., and Che Ani, F., 2022, "Effect of Alloy Particle Size and Stencil Aperture Shape on Solder Printing Quality," Microelectron. Int., **39**(2), pp. 81–90.
[14] Rusdi, M. S., Abdullah, M. Z., Chellvarajoo, S., Abdul Aziz, M. S., Abdullah, M. K., Rethinasamy, P., Veerasamy, S., and Santhanasamy, D. G., 2019, "Stencil Printing Process Performance on Various Aperture Size and Optimization for Lead-Free Solder Paste," Int. J. Adv. Manuf. Technol., **102**(9–12), pp. 3369–3379.
[15] Berthier, J., Brakke, K. A., Mermoz, S., Frétigny, C., and Di Cioccio, L., 2015, "Stabilization of the Tilt Motion During Capillary Self-Alignment of Rectangular Chips," Sens. Actuators A: Phys., **234**, pp. 180–187.
[16] Berthier, J., Brakke, K., Grossi, F., Sanchez, L., and Di Cioccio, L., 2010, "Self-Alignment of Silicon Chips on Wafers: A Capillary Approach," J. Appl. Phys., **108**(5), p. 054905.
[17] Krammer, O., Sinkovics, B., and Illes, B., 2007, "Studying the Dynamic Behaviour of Chip Components During Reflow Soldering," 30th International Spring Seminar on Electronics Technology (ISSE), Cluj-Napoca, Romania, May 9–13, pp. 18–23.
[18] Smith, G., 2017, "Impact of Stencil Foil Type on Solder Paste Transfer Efficiency for Laser cut SMT Stencils," Proceedings of SMTA International, Rosemont, IL, Sept. 17–21.
[19] Bath, J., Lentz, T., Smith, G., and Assembly, FCT, 2016, "An Investigation Into the Use of Nano-Coated Stencils to Improve Solder Paste Printing With Small Stencil Aperture Area Ratios," Proceedings of IPC Apex Expo, Las Vegas, NV, Mar. 15–17.
[20] Brakke, K. A., 1994, *Surface Evolver Manual*, Version 2.24, Mathematics Department, Susquehanna University, Selinsgrove, PA, p. 20.
[21] Najib, A. M., Abdullah, M. Z., Saad, A. A., Samsudin, Z., and Che Ani, F., 2017, "Numerical Simulation of Self-Alignment of Chip Resistor Components for Different Silver Content During Reflow Soldering," Microelectron. Reliab., **79**, pp. 69–78.
[22] Lai, Y., Pan, K., Cen, Y., Yang, J., Cai, C., Yin, P., and Park, S., 2022, "An Intelligent System for Reflow Oven Temperature Settings Based on Hybrid Physics-Machine Learning Model," Soldering Surf. Mount Technol., **34**(5), pp. 266–276.
[23] Lai, Y., Pan, K., Ha, J., Cai, C., Yang, J., Yin, P., Xu, J., and Park, S., 2022, "The Optimal Solution of Reflow Oven Recipe Based on Physics-Guided Machine Learning Model," 21st IEEE Intersociety Conference on Thermal and Thermomechanical Phenomena in Electronic Systems (iTherm), San Diego, CA, May 31–June 3, pp. 1–6.
[24] Lai, Y., Kataoka, J., Pan, K., Ha, J., Yang, J., Deo, K. A., Xu, J., et al., 2022, "A Deep Learning Approach for Reflow Profile Prediction," IEEE 72nd Electronic Components and Technology Conference (ECTC), San Diego, CA, May 31–June 3, pp. 2269–2274.
[25] Standard, J. E. D. E. C., 1995, "Thermal Shock," JEDEC, Arlington, VA, No. JESD22-A106-A.
[26] International Electrotechnical Commission, 1984, "Environmental Testing—Part 2-14: Tests—Test N: Change of Temperature," International Electrotechnical Commission, London, UK, No. IEC 60068-2-14: 1984
[27] Pan, J., 2014, "A Control-Chart-Based Method for Solder Joint Crack Detection," J. Microelectron. Electron. Packag., **11**(3), pp. 94–103.

[28] Pan, J., and Silk, J., 2011, "A Study of Solder Joint Failure Criteria," International Symposium on Microelectronics, International Microelectronics Assembly and Packaging Society, Long Beach, CA, Oct. 9–13, Vol. 2011, No. 1, pp. 694–702.
[29] Rajashekar, K., 2015, "Impact of Viscoelastic Material Characterization of PCB's on the Thermomechanical Properties of QFN Thick Package Under Thermal Cycling," Master's thesis, The University of Texas at Arlington, Arlington, TX.
[30] Steinberg, D. S., 2000, *Vibration Analysis for Electronic Equipment,* 3rd ed., Wiley-Interscience, Hoboken, NJ.
[31] Engelmaier, W., 1983, "Fatigue Life of Leadless Chip Carrier Solder Joints During Power Cycling," IEEE Trans. Compon., Hybrids, Manuf. Technol., **6**(3), pp. 232–237.
[32] Kang, M.-S., Kim, D.-S., and Shin, Y.-E., 2019, "The Effect of Epoxy Polymer Addition in Sn-Ag-Cu and Sn-Bi Solder Joints," Materials, **12**(6), p. 960.
[33] Han, C., and Song, B., 2006, "Development of Life Prediction Model for Lead-Free Solder at Chip Resistor," 8th Electronics Packaging Technology Conference, Singapore, Dec. 6–8, pp. 781–786.
[34] Cai, C., Xu, J., Wang, H., and Park, S. B., 2021, "A Comparative Study of Thermal Fatigue Life of Eutectic Sn-Bi, Hybrid Sn-Bi/SAC and SAC Solder Alloy BGAs," Microelectron. Reliab., **119**, p. 114065.
[35] Romdhane, E. B., Roumanille, P., Guédon-Gracia, A., Pin, S., Nguyen, P., and Frémont, H., 2021, "Early Microstructural Indicators of Crack Initiation in Lead-Free Solder Joints Under Thermal Cycling," 71st Electronic Components and Technology Conference (ECTC), San Diego, CA, June 1–July 4, pp. 2293–2301.
[36] Pan, K., Ha, J. H., Wang, H., Xu, J., and Park, S. B., 2020, "The Effect of Solder Paste Volume on Solder Joint Shape and Self-Alignment of Passive Components," IEEE 70th Electronic Components and Technology Conference (ECTC), Orlando, FL, June 3–30, pp. 1289–1297.
[37] Pan, K., Ha, J. H., Wang, H. Y., Veeraraghavan, V., and Park, S. B., 2019, "The Effect of Solder Paste Volume on Surface Mount Assembly Self-Alignment," Procedia Manuf., **38**, pp. 1381–1393.